ORIGINAL PAPER

Quasi-static in-plane behavior of full-scale unreinforced masonry walls retrofitted using ferro-cement overlay

Abul Hasnat[1] · Raquib Ahsan[1] · S. M. Yashin[2]

Abstract

This study presents an experimental investigation on the behaviour of in-plane loaded Unreinforced Masonry (URM) wall retrofitted with ferrocement technology. Quasi-static cyclic tests on full-scale URM walls have been performed. Unreinforced masonry walls were built with clay bricks and were placed on a reinforced concrete base slab. Wall assemblies had aspect ratio of 0.75. Walls were investigated for full ferrocement coverage with an extra joint lamination between the base slab and the wall panel. Steel wire meshes having opening size 12.5×12.5 mm were considered for ferrocement overlay. Behaviour of the strengthened walls under a combination of a vertical load and lateral reversed cyclic loading was compared to the control models to observe improvement of lateral load resistance capacity. Equivalent viscous damping of the walls was calculated to be within the range of 8–22%. The initial stiffness amplified up to 52% in case of samples retrofitted with ferrocement. Before formation of the first crack, the specimen retrofitted with ferrocement overlay withstood about two times more lateral load than the corresponding unretrofitted specimen. The post-cracking strength was greatly enhanced by the presence of ferrocement, which was almost 1.6 times for the failure load. Strengthening of the walls also improved the total energy dissipation by a factor ranging from 49 to 68%. The energy dissipation was almost 1.4 times higher than that of the control wall. Hysteresis loops showed higher ductility for retrofitted specimen than that of the control specimen. Unretrofitted specimen exhibited rocking failure pattern, whereas retrofitted specimen showed a combination of rocking and flexural mode of failure. Finally, it is concluded that retrofitting URM walls with ferrocement overlay may be a practical option as it can be applied easily by ordinary construction workers, at an affordable cost.

Keywords Unreinforced masonry (URM) wall · Quasi-static cyclic test · In-plane behaviour · Ferrocement overlay · Retrofitting

Introduction

Unreinforced masonry (URM) is one of the earliest and most commonly used construction materials in the world because of economy, aesthetics, architectural aspect, ease in construction, fire resistance and effective heat and sound insulation. In masonry buildings, URM walls are main load carrying components. URM buildings are primarily designed to carry only vertical loads. They are constructed with heterogeneous materials. A major portion of old buildings in many parts of the world are URM buildings. However, because of its low tensile strength, URM is not capable of carrying tensile forces and thus not suitable for large seismic loads.

The in-plane response of URM walls with and without retrofitting with ferrocement overlay is the focus of this paper. This study explores, through laboratory experiments, suitability of ferrocement overlay as a retrofitting material for masonry walls under lateral loading condition.

Acknowledging limitations of URM structures, in recent years interests of researchers have grown in developing methods for enhancing seismic performance of these structures. Quite a few approaches have been suggested, and a full overview of these techniques has been recorded by different researchers (El-Diasity et al., 2015; ElGawady et al., 2007; Failed, 2006a; Lizundia et al., 1997).

✉ Abul Hasnat
hasnat.ce@iut-dhaka.edu

1 Department of Civil Engineering, Bangladesh University of Engineering and Technology (BUET), Dhaka 1000, Bangladesh

2 Department of Civil Engineering, Islamic University of Technology, Dhaka, Bangladesh

Lizundia et al. (1997) developed strategies for improving the performance of repaired URM buildings (Lizundia et al., 1997). Different investigations carried out using grouted sleeve with shifted plastic hinge showed improved ductility level and thus enhancing seismic performance (Al-Jelawy et al., 2017, 2018; Haber et al., 2017). ElGawady et al. (2007) investigated that the single-side retrofitting made a big difference in the test specimens' lateral strength, stiffness, and energy dissipation (ElGawady et al., 2007). Though many seismic retrofitting techniques are possible for masonry structures, ferrocement technique has proven itself as both advantageous and cost-effective (Trikha et al., 1988). Only cement mortar is used in Ferrocement without coarse aggregates. Single or multiple layers of steel wire mesh are used as reinforcement. Ferrocement has become very popular because of availability of raw materials, cost-effective process and flexibility in construction (Kantharaju et al., 2001). Resistance of structures to fire, corrosion and earthquakes can be increased using ferrocement coating (Dass & Talwar, 2017). Ferrocement overlay can enhance in plane and out of plane ductility and strength of an unreinforced masonry wall (Prawel & Reinhorn, 1985). Strengthening of brick masonry columns using ferrocement was also found effective (Kumar & Sharma, 1976). Lateral load capacity of interior beam column joint retrofitted with ferrocement was found satisfactory too (Hossain, 2015). Experimental investigations conducted by some researchers showed that mortar overlays with some sort of reinforcement can be a powerful rehabilitation technique to strengthen masonry in plane properties (Alcocer et al., 1996; Irimies & Crainic, 1993; Jabarov et al., 1980; Kahn, 1984; Mander & Nair, 1994). The shotcrete considerably boosted the panels' in-plane shear strength, while minor quantities of steel reinforcement increased the panels' ductility (Kahn, 1984). Alcocer et al. (1996) concluded that using steel meshes and a mortar cover to jacket confined masonry walls is a viable strategy for enhancing earthquake resistance (Alcocer et al., 1996). Thus, a thin layer of Ferrocement (cement mortar together with wire mesh) overlay might be considered as a promising solution to improve the in-plane strength and ductility. It is important to investigate the behaviour of ferrocement retrofitted URM walls for different reinforcement arrangements and variations in other parameters that may affect strength and ductility.

The purpose of the present research is to explore the performance of ferrocement retrofitted unreinforced masonry wall under cyclic loading with various parameters. Investigation of the failure pattern of the specimens is also included in this study.

In previous experimental research studies, various types of experiments were conducted on the cyclic behavior of URM retrofitted with ferrocement (Ahsan et al., 2018; Asif et al., 2020, 2021; Failed, 2018). However, very few studies

have been conducted on full scale URM wall. To study the behavior of full scale unreinforced masonry (URM) walls, cyclic static incremental horizontal load is applied to test the wall under sustained vertical load. URM walls with 254 mm thick RC base are prepared. The thickness of wall is 127 mm, ferrocement overlay is applied on both faces. Wall is constructed with length and height of 3658 mm and 2743 mm, respectively (aspect ratio = 0.75). First, a wall is constructed without any ferrocement overlay and is used as the control specimen. Then, another wall is retrofitted with ferrocement with mesh size arrangement of 12 mm X 12 mm. Cyclic load–displacement behavior of the walls are then compared.

In-plane loaded wall response

Substantial testing programmes have been regulated on the in-plane response URM walls, recognizing failure modes, force–displacement relationships, and equations to anticipate their ultimate strength (Abrams, 1992; Calderini et al., 2009; Corradi et al., 2003; Failed, 1977; Magenes & Calvi, 1997; Priestley, 1985; Thurston & Beattie, 2009; Yi et al., 2006).

Numerous researchers have reported the different failure modes for in-plane URM walls (Calderini et al., 2009; Cattari & Lagomarsino, 2009; Lee et al., 2008; Magenes & Calvi, 1997; Mann, 1982; Marzahn, 1998; Priestley, 1985). In-plane behaviour modes of failure of a laterally loaded URM wall is shown in Fig. 1.

State of the art—strengthening methods of masonry wall

To enhance the strength of masonry walls against earthquakes, the researchers have put forward numerous new techniques (Ashraf et al., 2012; Hao et al., 2014; Jiang et al., 2015; Santis et al., 2016). Jiang et al. (2015) concluded that the lateral strength, stiffness, and energy-dissipation capacity of the bare RC frame rise dramatically with the inclusion of a rigidly linked masonry infill wall, whereas the displacement ductility ratio reduces significantly (Jiang et al., 2015). Santis et al. used a system consists of horizontal strips of ultra-high strength steel cords attached to the brickwork with hydraulic lime mortar, and transversal wall connectors put within the plaster layer which improved out-of-plane seismic capacity of masonry walls (Santis et al., 2016). Tang et al. (2017) experimented on reinforced masonry walls using steel mesh cement mortar splint and built masonry walls using mortars that had low strength (Tang et al., 2017). Two types of compound materials were used in some studies for increasing the strength of masonry walls (Bae et al., 2011; Capozucca, 2011; Deng et al., 2013). ElGawady et al. (2006) adopted steel mesh concrete slabs to reinforce the two surfaces of walls. The building dwellers rejected this method,
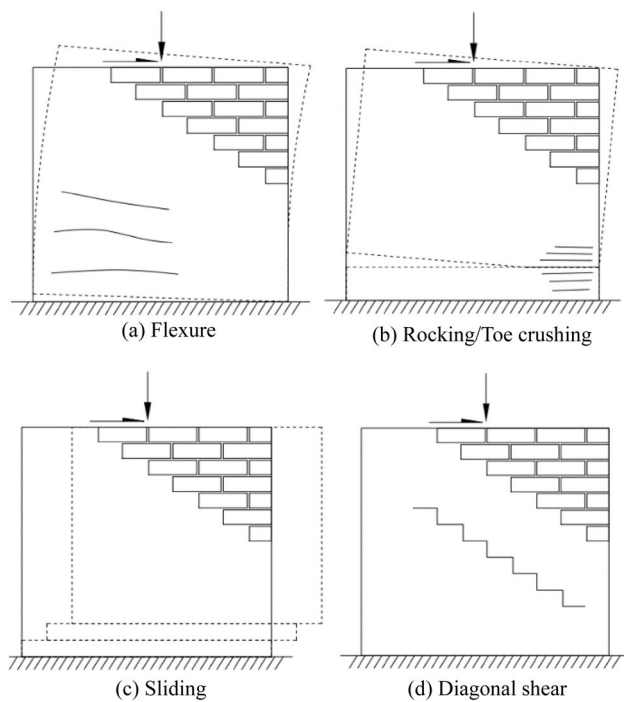
Fig.1 In-Plane Behaviour Modes of a Laterally Loaded URM Wall (Marzahn, 1998)

because the exterior decorative mortar of the walls needed to be discarded (Failed, 2006a). Maalej et al. (2010) experimented that Engineered Cementitious Composite (ECC)-strengthening systems are effective in raising URM walls' ultimate load-carrying capacity, improving their ductility, increasing their resilience to many low-velocity impacts, and minimizing rapid and, therefore, catastrophic failure (Maalej et al., 2010). Bae et al. (2011) evaluated the structural capability of masonry shear walls and the retrofitting impact of FRP sheets for in plane shear behavior were compared to the assessment technique for reinforced concrete beams retrofitted with FRPs (Bae et al., 2011). Mahmood et al. (2011) investigated in his study that fiber-reinforced polymer (FRP) systems significantly boosted the shear strength of in-plane loaded URM walls (Mahmood & Ingham, 2011).

Taghdi et al. (2000) and Farooq et al. (2014) investigated the consequence of using steel strip reinforcement on ductility and bearing capacity of masonry walls (Farooq et al., 2014; Taghdi et al., 2000). Moghaddam et al. (2004) and Jiang et al. (2015) conducted tests to analyse the seismic properties of walls that are strengthened using external steel encasing (Jiang et al., 2015; Moghaddam, 2004). Lattice steel plates were used in the research of Yu et al. (2014) and the effects of this strengthening method on masonry properties such as strength, ductility and rigidity were investigated (Jiang & Yongming, 2014). This technique cannot be applied on interior transverse walls. In the study of Kadam et al.

(2014), reversed cyclic quasi-static loading tests were done on masonry walls that are not strengthened and then, the strength of the walls was increased using polymer mortar splint and high-strength steel wire (Kadam et al., 2014).

Ferrocement

Ferrocement consists of cement mortar and steel wire mesh as the main reinforcing material for confinement of the structural elements (A. C. I., 1997; Naaman, 2000; Nassif & Najm, 2004).

Retrofitting of URM wall using ferrocement

The response of unconfined URM walls retrofitted with ferrocement was investigated under various types of cyclic loading by Ahsan et al. (2018) (Ahsan et al., 2018).

Two full-scale brick masonry walls under quasi-static load, one confined and one unreinforced, to investigate in-plane lateral load behavior of walls prior to and following retrofitting was presented by Ashraf et al. (2011) (Ashraf et al., 2012).

The usage of ferrocement jacketing technique as a productive method to enhance structural performance of unreinforced masonry walls was demonstrated by Mustafaraj et al. (2016) (Mustafaraj & Yardım, 2016).

It was noticed that ferrocement jacketing made a significant enhancement in deformation capacity and shear strength for unreinforced masonry walls. El-Diasity et al. (2015) did in-plane cyclic loading experiments on retrofitted confined masonry walls (El-Diasity et al., 2015). GFRP systems as well as low-cost ferrocement and were used in the test. The research to explore the potency of retrofitting damaged masonry walls with in-plane strengthening by application of a reinforced mortar coating and cement paste injected into cracks was presented by Irimies and Crainic (1999) (Irimies & Crainic, 1993).

Ashraf et al. (2012) used cement based grout injection and ferrocement overlay as retrofitting material to investigate the response of a full scale unreinforced damaged brick masonry building under cyclic loading (Ashraf et al., 2012). An experimental program designed to explore the potency of retrofitting damaged unreinforced clay unit masonry walls with a reinforced mortar coating was presented by Jabarov et al. (1980) (Jabarov et al., 1980). A test study on URM building retrofitted with ferrocement layers was done by Fauzan et al. (2018) (Ismail et al., 2018). An experimental program was presented by Prawel and Reinhorn (1985) to explore the effectiveness of ferrocement coatings for the in-plane rehabilitation of unreinforced masonry walls (Prawel & Reinhorn, 1985). The results of a series of experiments done on URM walls to find the test values for masonry

stiffness and shear strength was reported by Corradi et al. (2008) (Corradi et al., 2008).

Quasi-static cyclic testing of masonry structure

Calvi et al. (1997) observed that quasi-static tests lean towards indicating lower load resistance in comparison with dynamic tests (Magenes & Calvi, 1997) and are, therefore, usually taken into account to be conventional for seismic assessment as URM displays rate-dependent behavior, thereby crack propagation may arise during implementation of a sustained load.

Axial load on masonry wall

Determining anticipated service loads is the primary step in the design of any engineered masonry structure. The necessary strength of the masonry can be determined once these loads are established. Prism Test method was recommended in masonry wall chapter of Bangladesh National Building Code (BNBC) 1993 as a sensible procedure to verify masonry compressive strength (Code & BNBC., 1993). Allowable compressive Stress (axial load) on Unreinforced masonry walls as per BNBC 1993 is given below:

$$F_a = \frac{f'_m}{5}\left[1 - \left(\frac{h'}{42t}\right)^3\right] \tag{1}$$

where F_a = allowable average axial compressive stress. f'_m = specified compressive strength of masonry. h' = effective height of column. t = effective thickness of column.

Viscous damping ratio of cyclic test

In this study, equivalent viscous damping is calculated based on the theorem of Hose and Seible (1999):

$$\xi_{eq} = \frac{1}{4\pi}\left(\frac{E_{d1}}{E_{s1}} + \frac{E_{d2}}{E_{s2}}\right) \tag{2}$$

The equivalent viscous damping ratio, ξ_{eq}, is obtained in Equation (2) for the full asymmetric cycle at a specific force level. It is again clarified in Fig. 2. In Fig. 2, area E_{d1} denotes the damping energy loss or energy input for the push half cycle of the idealized force–displacement loop. Likewise, area E_{d2} portrays the energy loss for the pull half cycle. E_{s1} and E_{s2} is defined in Fig. 2 by the hatched regions. In an equivalent linear elastic system, strain energy stored for the push and pull half cycles, respectively, which is represented by the above theorem.

Experimental program

Using full scale clay brick units, an unreinforced masonry wall was built. A 254 mm RC base slab was supporting the wall. The measurements of the wall were chosen as such that goes with the Hydraulic Testing Machine. 127 mm and 2743 mm were, respectively, the thickness and height of the wall. The length of the wall was around 3658 mm with an aspect ratio of 0.75. Figure 3 shows standard details of the tested walls. The wall was tested under a combination of a lateral cyclic loading and a constant vertical load with force controlled loading pattern till failure. To obtain sustained

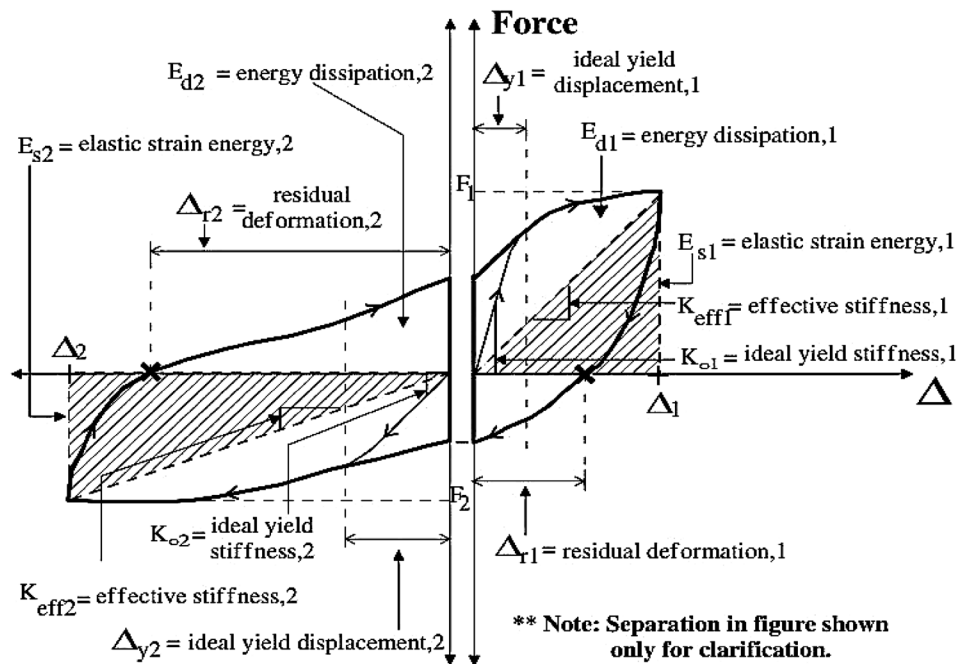**Fig. 2** Equivalent Viscous Damping Ratio (ξeq) for Asymmetric Hysteresis Loops (Hose & Seible, 1999)
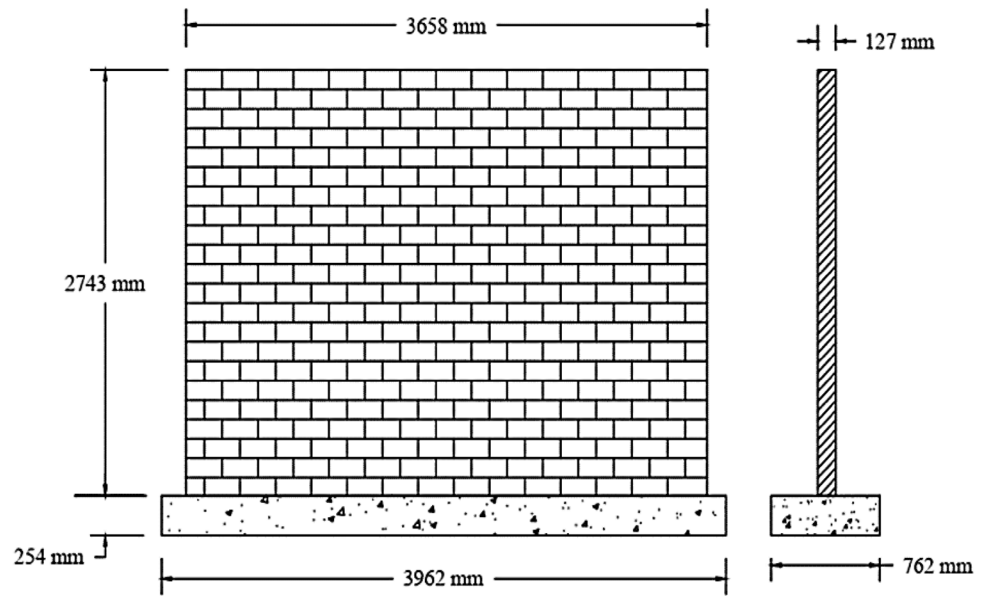
Fig. 3 Details of the tested wall

Table 1 Crushing strength test result of bricks

Serial No	Width (mm)	Length (mm)	Observed Load (KN)	Actual Load (KN)	Area (mm2)	Stress (MPa)	Average (MPa)
1	113	109	238	239	12,345	19	19
2	116	110	206	208	12,696	16	
3	122	109	308	309	13,316	23	
4	113	113	208	209	12,776	16	
5	113	113	276	277	12,776	22	

uniform gravity load, a steel joist was placed on top of the wall. Loads were applied on that steel joist. Besides, to conform uniformity of applied load, horizontal quasi-static load was applied on a steel plate placed on side face of the wall.

Material properties

Brick

Local bricks having frogmarks on both sides were used to construct the walls. Full scale bricks were used. The normal size of bricks was $240 \times 115 \times 70$ mm. Compressive (crushing) strength test was conducted accordance with ASTM C 67-09. Table 1 shows the results crushing strength test of bricks using the standard code procedure.

Fine aggregate

Coarse Sylhet sand and fine riverbed sand were used for specimens. Gradation of both sands satisfies the ASTM standard conditions of specification C136. For base slab construction, Sylhet sand was used and for masonry wall
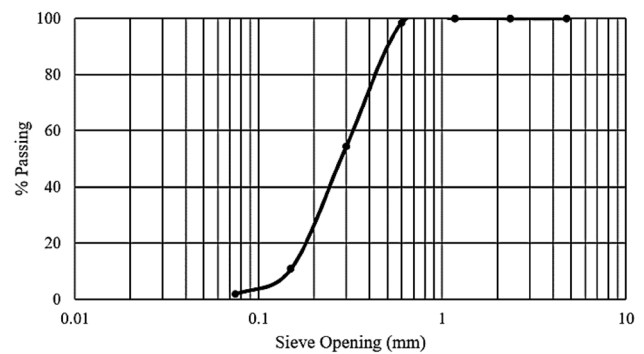

Fig. 4 Gradation curve of local sand

construction, riverbed sand was used. Gradations of these sands are shown in Figs. 4 and 5. Properties of fine aggregate are shown in Table 2

Coarse aggregate

Coarse aggregates (brick chips) were prepared from manually crushing first class bricks. 19 mm down grade brick
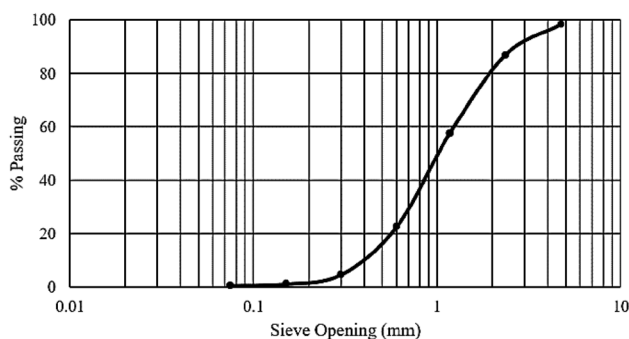
Fig. 5 Gradation curve of Sylhet sand

chips were collected for the model preparation. Properties of coarse aggregate are shown in Table 2.

Cement

For the control and retrofitted specimens CEM-I (Ordinary Portland Cement) was used. In CEM-I cement, 95 to 100% is clinker and additional constitutes are 0 to 5%. Used CEM-I Conform 52.5 N Grade of BDS EN 197–1:2003(BSTI, 2022).

Mortar

The compressive strength test of mortar was conducted according to the ASTM standard C109. Type-M2 mortar with cement: sand ratio of 1:4 was used to prepare the model. For each mortar casting 50 mm (2 inch) standard cubes were tested. The 7 day, 14 day and 21 day average compressive strength of mortar were tested to be 5.6 MPa, 9 MPa and 10 MPa, respectively.

Prism test

To determine the strength of the masonry, prisms were tested in compression. ASTM C1314 Standard Test Methods for Masonry Prisms Compressive Strength was followed. Prisms were prepared by assembling five brick masonry units, one on top of the other, using mortar as the bonding material, representative of those being used in the samples, in the contact surface of the masonry units. After curing for a period of 28 days, the prisms were tested in the laboratory. All the

prisms were capped with a fine layer of dental plaster of 1–2 mm coating to level the contact surface between the platens and specimen face of the testing machine before testing. The average compressive strength of prism was found to be 4.4 MPa.

Concrete

In concrete mix 19 mm down grade brick chips were used with coarse aggregate and Sylhet sand were used. The water–cement ratio of 0.40 was used. Fine aggregate to total aggregate volumetric ratio (S/A) was kept at 0.4. Detailed mix design for the preparation of concrete mixture is shown in Table 3.

Wire mesh

As it is mentioned earlier, 18 gauge wire mesh was used for ferrocement lamination. For ferrocement overlay, a single layer of 18-gauge wire mesh with 12.5 mm × 12.5 mm opening was used to retrofit specimens. Woven type wire mesh was used. The mesh was of mild steel. No external bonding agent was used at the interface of wire mesh and URM wall.

Test specimen preparation

Following the practical construction practice, wall specimen was formed in three different steps. At first, the base slab was casted. Then, right after curing of base slab the brick masonry was erected. Finally, ferrocement overlay was applied to wrap the walls to be retrofitted. The steps for preparation of the specimens are described below:

Base slab construction

A base slab with a cross section of 762 × 254 mm and span length of 3963 mm, was at first constructed horizontally. To resist the flexural tension during uplifting of walls, 16 mm

Table 3 Concrete mix design

W/C	S/A	Mixture Proportion, Kg/m^3			
		Cement	Water	Coarse Aggregate	Fine Aggregate
0.4	0.4	400	160	821.85	680.73

Table 2 Properties of coarse and fine aggregates

Type of Aggregate		Specific gravity	Absorption (%)	Unit weight (SSD) Kg/m^3	Abrasion
Fine Aggregate	Sylhet Sand	2.46	3%	1574	-
	River Bed Sand	2.24	1.27%	1360	-
Coarse Aggregate	Brick Chips	1.98	13.24%	1209	31.2%

diameter deformed bars were placed @ 100 mm c/c in both transverse and longitudinal directions. Proper compaction was ensured using a vibrator. 25 mm thick timber planks were used for the formwork. For curing, wet jute hessian was used to cover the entire sample. Every day, the beams were cured 3 times with water up to 28 days. Figures 6 and 7 show the construction sequences.

URM wall construction

Brick walls were constructed on the base slab after 28 days of construction of base slab. Three cubes were collected for testing purposes for each mixing of mortar. For curing, wet jute hessian was used to wrap the walls. Water was applied two times a day up to 14 days. The surface was levelled with wooden trowel and the unretrofitted walls were plastered with mortar.

Retrofitting work

The bare URM reference specimen was first tested without allowing collapse. The reference specimen was then retested after strengthening it using wire mesh. 18 gauge wire mesh consisting of 12.5 mm × 12.5 mm opening was employed for the retrofitting purpose. Epoxy grout was used to close the cracks induced during the first run of the test. The white wash was taken off of the model before retrofitting. The whole length of the wall was wrapped with the

Fig. 6 Reinforcement arrangement for base slab

Fig. 7 Base slab after casting

wire mesh. Rawl bolt was used to attach the wire mesh to the wall. Then, one wall was plastered and another wall was kept uncovered. Cement grout was used with admixture to achieve a faster gain in strength of the plaster. Retrofitted sample was retested after 8 days. The application process of wire mesh and plastering is shown from Figs. 8, 9. Wire mesh was used on the wall only. The wire mesh was not extended to the base.

Instrumentation

The deformations of the specimen were measured with Linear Variable Displacement Transducers (LVDTs) and Laser Displacement Sensors (LDSs) (Fig. 10). A computer controlled data acquisition system was used to record the information read by each device. To acquire the deformation data in the direction of loading, the data-acquisition system calculated the data at a sampling rate of 200 Hz. Capacities of the LDSs and LVDTs are summarized in Table 4 and their locations on the retrofitted sample and on the reference sample are illustrated in Fig. 10. All the sensors were used to measure in-plane lateral deformation.

Instruments were calibrated to output displacement. Instruments were defined such that tension (extension) was measured as negative displacement (pull cycle) and

Fig. 8 Wire mesh confinement processing

Fig. 9 Wire mesh on plastered wall

from 40x–50 mm, and the test was discontinued at 50 mm wall tip displacement, resulting in a wall tip drift of 2.0%.

Experimental setup

At the top of the wall, a hydraulic-powered jack was used to impose the horizontal shear force. The strong-wall of the laboratory was utilized as a reaction point. A steel loading beam was placed and mortared to transfer loads on the top of the wall via friction in both push and pull cycles. The base was bolted down to restrain the wall from sliding as the wall was built on a base. To prevent overturning of the base slab during test, the base slab was fixed by pre-tensioned bolts anchored to the reaction floor.

The walls were tested until failure under a combination of constant vertical load and in-plane cyclic lateral load. The test setup of the walls is shown in Fig. 10. A single point load was distributed by a rigid steel I-beam laid on top of wall. To evaluate compressive strength of masonry, f'_m, prism tests were conducted.

Based on the prism test results of the masonry specimens, the value of the vertical load was fixed. According to the formula set by BNBC 2020 the allowable axial compression carrying capacity of the masonry wall is a function of f'_m.

20% of the allowable compression was applied vertically. According to the BNBC provisions, the permissible axial capacity of URM wall was determined as 30 ton. The lateral cyclic load was implemented with a 50-ton hydraulic jack. After curing, the specimen was carried to set into the

compression was measured as positive displacement (push cycle).

Loading scheme

Figure 11 shows the loading scheme used in the tests This quasi-static loading history was adopted by Russell et al. (2007) to conduct cyclic test on URM walls (2005). In this loading scheme, the push direction was designated as positive and the pull direction as negative. This displacement-controlled quasi-static process was applied to observe the failure and damage mechanisms and to describe the non-uniform pattern of damage in the wall. In every direction, the wall went through displacements of 1 mm or 0.04% drift. Then, the displacements were raised by increments of 1 mm per cycle until it achieved 10 mm displacement. The increments were 2 mm or 0.08% drift per cycle from displacements of 10 mm–32 mm, and 4 mm or 0.16% drift from 32 to 40 mm. The increments were 5 mm or 0.2% drift per cycle

Fig. 10 Schematic diagram of experimental setup with the Locations of LVDTs & LDSs
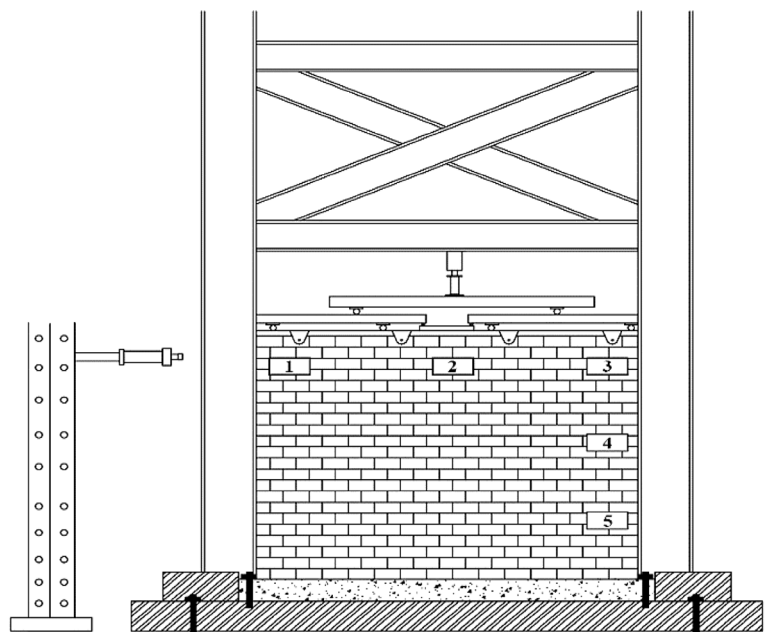
Table 4 LVDTs and LDSs locations

LVDTs & LDSs No	Range, mm
1	150–2000
2	1500–2000
3	150–800
4	150–800
5	150–2000

hydraulic testing machine cautiously to avoid any significant damages.

An overhead crane and a trolley were used to carry the specimens. When the specimen was set up then the hydraulic jacks were placed into position. A stiff steel distributor joist was laid in the wall to distribute the vertical loads as uniformly as possible. One vertical jack was placed at middle of the wall over the steel joist.

To commence each test, the vertical hydraulic jacks set at their fixed position over steel joist were first loaded to a 10 ton force. Some views of the experimental setup are shown from Figs. 12, 13 14.

Fig. 11 Loading history applied in wall
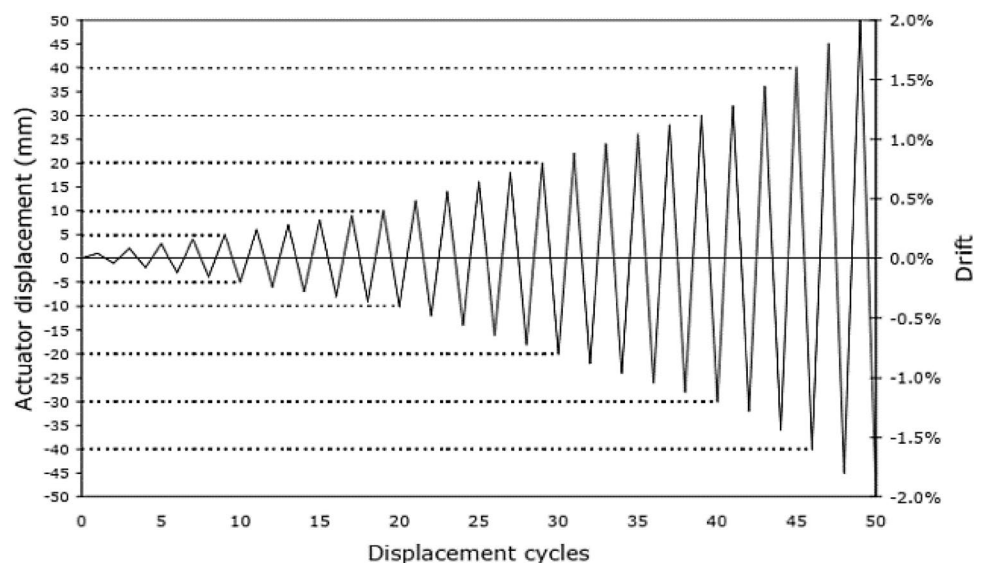
Fig. 12 Setup of wall test

Fig. 13 Actuator with strong wall

Results and discussion

Quasi-static cyclic test was conducted to determine the load versus displacement (hysteresis) behavior under pre-defined displacement histories. This section summarizes the qualitative and quantitative experimental results from the test specimens (Fig. 15).

Fig. 14 Hydraulic jack over wall

Loads corresponding to the imposed displacements were recorded for producing the quantitative results. They are plotted in a graphical form to have a clear understanding of the scenario. In addition, certain parameters such as energy dissipation, stiffness degradation, ductility and percentage of hysteretic damping are also compared here on the basis of load deformation response.

Crack pattern of the control specimen (WC)

Different types of cracks were observed in quasi-static test including hairline cracks to large cracks, which ultimately resulted in severe damage and mortar fallout. The failure pattern for the un-retrofitted wall is shown in Fig. 16. Moderate to severe damage in one end of the wall near the base indicates that the wall went through large rotation, which defines typical rocking failure.

The first crack appeared at the wall-base slab connection. The crack first initiated at base slab wall interface at the negative 3rd cycle loading with 4.42 ton loads and corresponded to a horizontal displacement of 0.54 mm. Later, the wall followed a failure path (Fig. 17) in which it failed at positive 7th cycle loading at right side with 13.1 ton loads corresponding to a horizontal displacement of 7.45 mm.
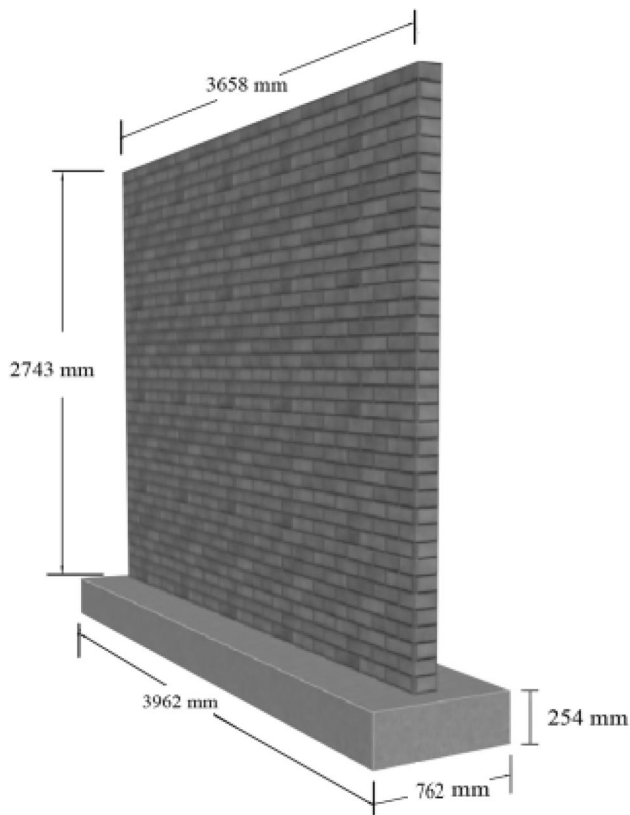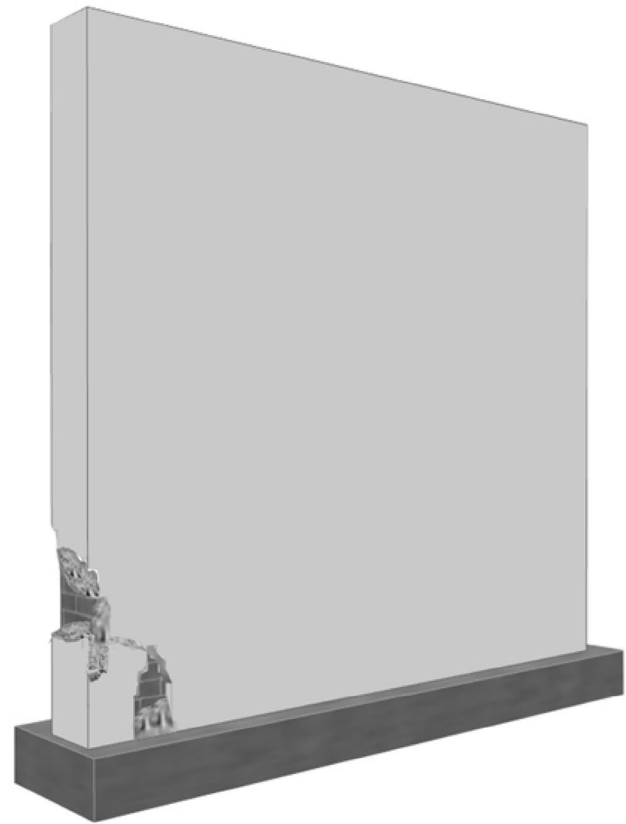
Fig. 15 Test wall geometry

Fig. 16 Failure pattern of WC

Crack pattern of the retrofitted specimen (WF)

Figure 18 indicates the cracks of retrofitted sample after applying loads. The first crack generated at the wall-base slab connection at positive 4th cycle loading with 9.38 ton loads corresponding to a horizontal displacement of 1.1532 mm. The first crack, propagated vertically up the head joint, stepping around the bricks.

The wall finally failed at positive 8th cycle loading with 19.6 ton loads corresponding to a horizontal displacement of 7.67 mm. Propagation of crack occurred along the brick–mortar interface which is common for URM. In general, this happens at a place where low ratio of the mortar compressive strength to the brick compressive strength exists.

Failure modes of URMs

Un-retrofitted specimens failed in rocking mode. Failure mode of ferrocement strengthened wall was initially a flexure induced mode and with increased lateral displacement developed into a combined flexure/rocking failure mode.
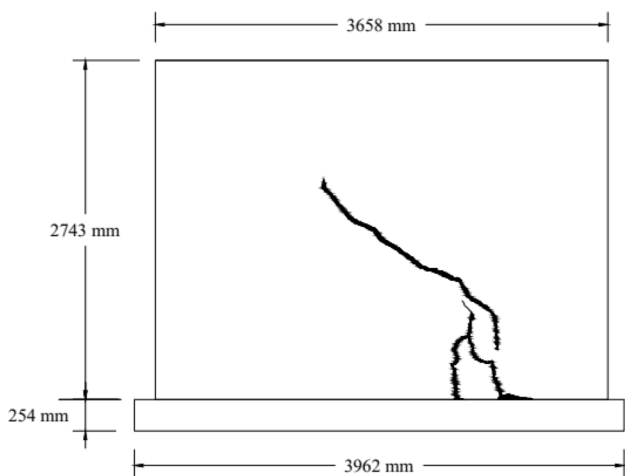

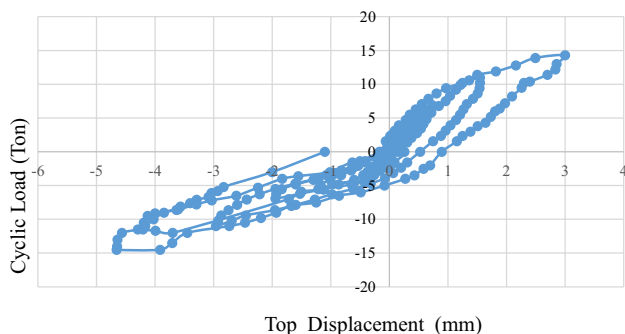**Fig. 17** Loading history applied in wall

Fig. 18 Crack pattern for WF

Fig. 20 Relationship between load and lateral deformation response of specimen WF

Fig. 19 Relationship between load and lateral deformation response of specimen WC

Fig. 21 Hysteresis damping percentage

Hysteresis loop

The displacement plotted was measured at the top of the walls. Cyclic behaviour of the walls is derived from the hysteresis loops (Figs. 19 and 20), which indicate the cyclic behaviour of the walls to be highly inelastic. For seismic performance, this type of behaviour is beneficial. Hysteretic loops of specimen WC shows moderate stiffness and moderate energy dissipation. It also indicates strength degradation with increasing displacement.

On the other hand, characteristics of a flexure failure mode are indicated from the force–displacement plot of the specimen WF, as shown in Fig. 20.

The large hysteretic loop is consistent with the observed wall failure mode. Same consistency is observed for stiffness degradation and severe strength after peak lateral strength was reached. Highly non-linear characteristics are exhibited by both tested samples. The failure mode dominated the measured hysteretic shape of the walls.
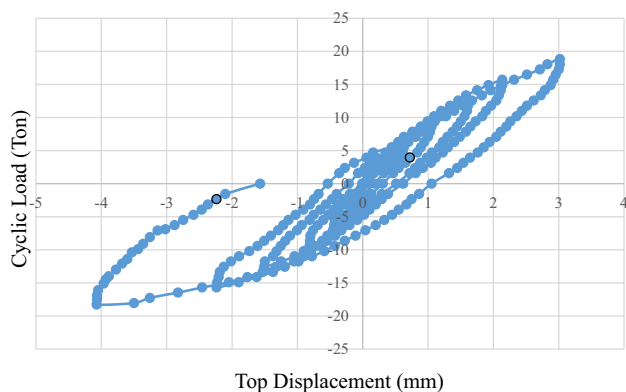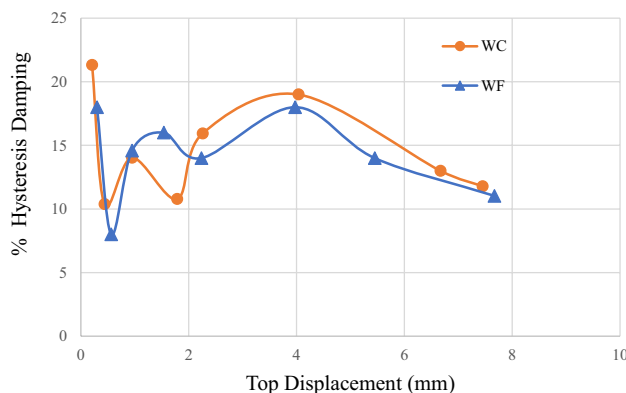
Hysteresis percentage damping

Due to hysteretic energy dissipation, the walls exhibited highly inelastic cyclic behavior. The hysteretic damping is shown in Fig. 21, which is plotted against lateral top displacement for walls. Behavior of specimen is not linear. Since masonry is not homogenous and anisotropic material, it is expected. For the wall, the hysteretic damping ranges from 8 to 22%.

Stiffness degradation

It is evident from stiffness degradation curves of both the walls (Fig. 22) that both underwent a moderate degree of stiffness and strength degradation. Various irreversible sources of damage likely resulted the overall degradation. The secant stiffness was used to evaluate the variation in stiffness of wall with increased top displacement and loading. Noted that, secant stiffness is defined as the ratio between the lateral resistance and the corresponding top lateral wall displacement At a certain displacement level, stiffness of a cycle was assessed by considering the average of stiffness in the negative and positive loading directions
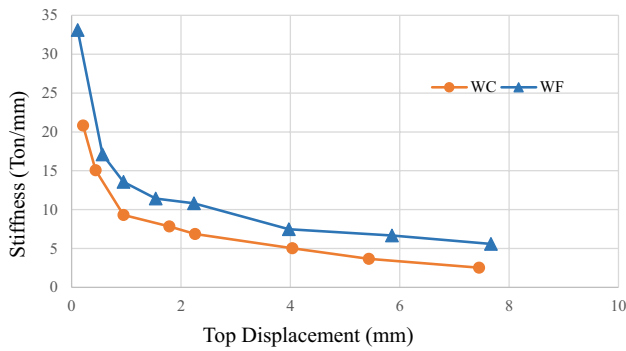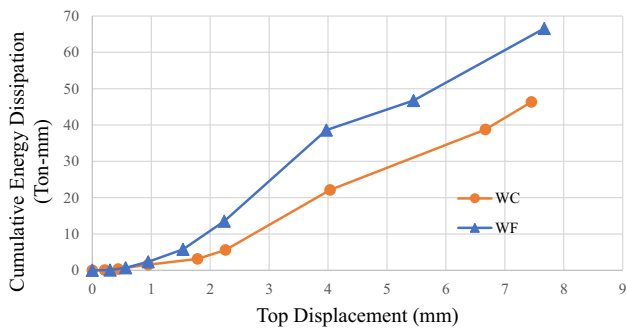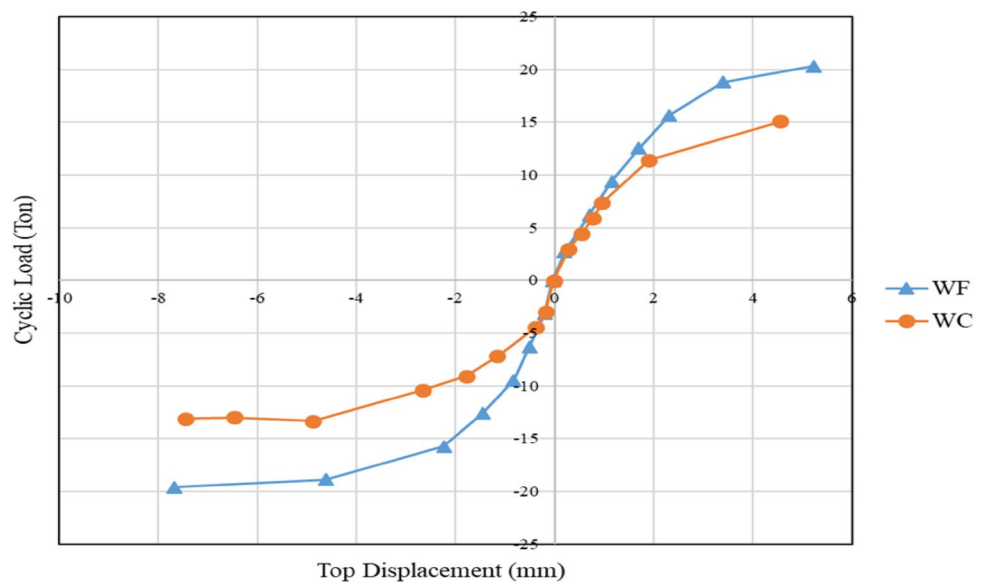
Fig. 22 Stiffness degradation

Fig. 23 Cumulative energy dissipation

(El-Diasity et al., 2015). WF had higher stiffness initially later had the higher capacity. Implementation of increasing displacement and the damage accumulated from repeated cyclic deformation resulted in a moderate degree of stiffness and strength degradation in all specimens.

Cumulative energy dissipation

Integrating the hysteresis loop (force–displacement) numerically for each complete loading cycle, the energy dissipation capacities of both the walls were determined. With the increment of drift, energy dissipation was increased, which was the general trend for both the walls (Fig. 23).

Envelope curve

Envelope load–deformation curve for the walls are shown in Fig. 24. Conspicuously both retrofitted and unretrofitted walls showed ductility to some extent. This ductility was shown in the ultimate load capacity region. The ductility indicates a wall's enduring capability of maintaining a relatively constant load resistance with continuous deformation. With respect to seismic resistance, such attribute is desirable. Gradual redistribution of internal bending moment from diagonal cracks to vertical cracks along the edges results in such ductility. At this phase of testing, the vertical edge cracks were only partially developed, while the diagonal cracks were fully developed in both the test walls. Therefore, observed crack patterns also support the ductility characteristics of the walls.

Load at first cracking and failure

Figures 25 and 26 represent a summary of the results in terms of first cracks and final cracks of all the specimens. It is evident from the figures that the retrofitted specimen performed better than the unretrofitted one in terms of first crack appearance and specimen failure.
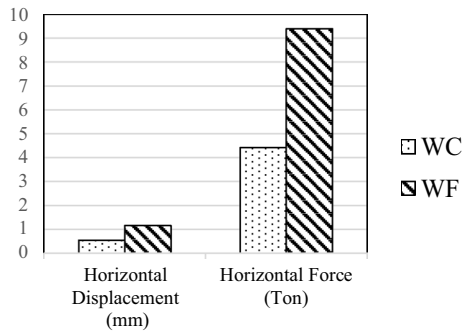
Fig. 24 Envelope curves

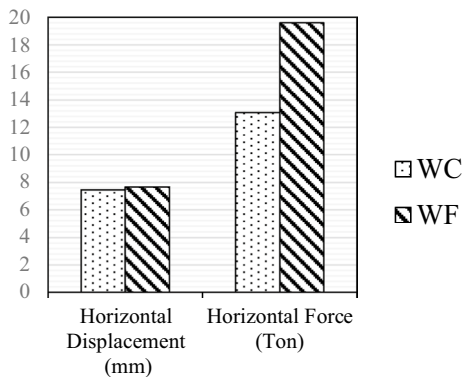**Fig. 25** Summary Results of First Crack

Fig. 26 Summary Results of Specimen Failure

Conclusions

Behaviour of a URM wall retrofitted by ferrocement overlay under cyclic loading test was investigated. A quasi-static cyclic test on full-scale wall has been performed on URM wall. The main outcome of this test has been the demonstration that URM wall possesses substantial post-cracking strength and displacement capacity with ferrocement lamination Due to hysteretic energy dissipation, the walls exhibited highly inelastic cyclic behaviour. Equivalent viscous damping was calculated to be within the range of 8–22%. In this range, in every point, retrofitted sample showed much more energy conservation. Under cyclic loading stiffness of the specimens decreased gradually. However, for the retrofitted sample, stiffness of the specimen did not degrade at the same rate. The initial stiffness is amplified up to 52% by retrofitting with ferrocement. Fully ferrocement encased walls showed the highest increase in terms of stiffness. Significant stiffness and strength degradation in the force–displacement behaviour was caused by the progressive damage accumulated by the walls during the course of the cyclic tests.

Before formation of first crack, the specimen retrofitted with ferrocement overlay experienced about two times more lateral load than the corresponding unretrofitted specimen. By the presence of ferrocement, the post-cracking strength was shown to be greatly increased, which is almost 1.6 times for failure load. The strengthening also improves the total energy dissipation by a factor ranging from 49 to 68% for walls. The energy dissipation is almost 1.4 times higher than that of control for walls. Ductility is increased by retrofitting the wall with ferrocement. Hysteresis loops showed higher ductility for retrofitted specimen than that of reference specimen. Unretrofitted specimen exhibited rocking failure pattern, whereas retrofitted specimen showed rocking and to some extent flexural mode of failure. Finally, local construction workers can easily apply the ferrocement mesh, at an economical cost.

Declarations

References

A. C. I. (ACI), State-of-the-Art report on ferrocement, ed. manual of concrete practice: ACI Committee 549, 1997.

Abrams, D. P. Strength and behavior of unreinforced masonry elements, 1992.

Ahsan, R., Asif, M. M., & Alam, M. Z. (2018). Performance analysis of ferrocement retrofitted masonry wall units under cyclic loading. *International Journal of Civil and Environmental Engineering, 12*(10), 1028–1033.

Alcocer, S., Ruiz, J., Pineda, J. and Zepeda, J. "Retrofitting of confined masonry walls with welded wire mesh," in *Proceedings of the Eleventh World Conference on Earthquake Engineering*, 1996.

Al-Jelawy, H., Haber, Z. and Mackie, K. Grouted splice precast column connections with shifted plastic hinging, in *16th World conference on earthquake—16WCEE*, 2017, pp. 9–13.

Al-Jelawy, H., Mackie, K., and Haber, Z. Experimental and numerical studies on precast bridge columns with shifted plastic hinging, in *Eleventh US national conference on earthquake engineering*, 2018, pp. 25–29.

Alam, M. A. Md. Mahir & Ahsan, Raquib., A study on the performance of ferrocement retrofitted masonry wall units under cyclic loading, presented at the 4th International Conference on Advances in Civil Engineering 2018 (ICACE 2018), Bangladesh, 2018, 2018, 451–455.

Ashraf, M., Khan, A. N., Naseer, A., Ali, Q., & Alam, B. (2012). Seismic behavior of unreinforced and confined brick masonry walls before and after ferrocement overlay retrofitting. *International Journal of Architectural Heritage, 6*(6), 665–688.

Asif, M., Alam, M., and Ahsan, R. (2020) An experimental investigation of ferrocement retrofitted masonry wall units subjected to cyclic loading, in *5th International Conference on Advances in Civil Engineering*.

Asif, M. M., Alam, M. Z., and Ahsan, R. Experimental study on behavior of ferrocement retrofitted unconfined URM wall under

cyclic loading, *Asian Journal of Civil Engineering,* pp. 1–16, 2021.

Bae, B., Park, B., Choi, H. K., and Choi, C. S. Retrofitting effect of unreinforced masonry walls using FRPs, in *Key Engineering Materials*, 2011, vol. 452: Trans Tech Publ, pp. 765–768.

BSTI, "BDS EN 197–1:2003" 2005

Calderini, C., Cattari, S., & Lagomarsino, S. (2009). In-plane strength of unreinforced masonry piers. *Earthquake Engineering & Structural Dynamics, 38*(2), 243–267.

Capozucca, R. (2011). Experimental analysis of historic masonry walls reinforced by CFRP under in-plane cyclic loading. *Composite Structures, 94*(1), 277–289.

Cattari, S. and Lagomarsino, S. (2009) Modelling the seismic response of unreinforced existing masonry buildings: a critical review of some models proposed by codes, in *Proc. 11th Canadian masonry symposium, Toronto, Ontario.*

Bangladesh National Buidling Code, BNBC. (1993), H. a. B. R. I. a. B. S. a. T. Institute, 1993.

Corradi, M., Borri, A., & Vignoli, A. (2003). Experimental study on the determination of strength of masonry walls. *Construction and Building Materials, 17*(5), 325–337.

Corradi, M., Borri, A., & Vignoli, A. (2008). Experimental evaluation of in-plane shear behaviour of masonry walls retrofitted using conventional and innovative methods. *Masonry International, 21*(1), 29.

Dass, G. and Talwar, M. Review Paper on Ferrocement in Construction, *International Journal of Advanced Research in Computer Science,* vol. 8, no. 4, 2017.

De Santis, S., et al. (2016). Seismic performance of masonry walls retrofitted with steel reinforced grout. *Earthquake Engineering & Structural Dynamics, 45*(2), 229–251.

Deng, M., Gao, X., & Liang, X. (2013). Experimental investigation on aseismic behavior of brick wall strengthened with ECC splint. *Engineering Mechanics, 30*(6), 168–174.

El-Diasity, M., Okail, H., Kamal, O., & Said, M. (2015). Structural performance of confined masonry walls retrofitted using ferrocement and GFRP under in-plane cyclic loading. *Engineering Structures, 94*, 54–69.

ElGawady, M. A., Lestuzzi, P., & Badoux, M. (2007). Static cyclic response of masonry walls retrofitted with fiber-reinforced polymers. *Journal of Composites for Construction, 11*(1), 50–61.

Page, A. W. (1977) The in-plane deformation and failure of brickwork, University of Newcastle.

ElGawady, M., Lestuzzi, P., and Badoux, M. "Retrofitting of masonry walls using shotcrete," in *2006a NZSEE Conference, Paper*, 2006a, vol. 45.

Hua, P., Hongxing, Q., and Xingbin, Z. (2006b) Experimental study on seismic reinforced of brick masonry walls with carbon fiber reinforced polymer (CFRP)[J], *Building Structure,* vol. 7.

Farooq, S., Shahid, I., & Ilyas, M. (2014). Seismic performance of masonry strengthened with steel strips. *KSCE Journal of Civil Engineering, 18*(7), 2170–2180.

Haber, Z. B., Mackie, K. R., & Al-Jelawy, H. M. (2017). Testing and analysis of precast columns with grouted sleeve connections and shifted plastic hinging. *Journal of Bridge Engineering, 22*(10), 04017078.

Hao, W., Shichun, Z., & Hu, X. (2014). Study on seismic strengthening design of masonry school building based on failure mechanism control. *China Civil Engineering Journal, 47*(3), 12–18.

Hose, D. Y. and Seible, F. "Performance Evaluation Database for Concrete Bridge Components and Systems under Simulated Seismic Loads," *PEER Report 1999/11* 1999. [Online]. https://peer.berkeley.edu/sites/default/files/9911_y._hose_f._seible_.pdf.

Hossain, T. Experimental investigation on performance of interior beam column joints retrofitted with ferrocement and polyester fiber reinforced concrete, 2015.

Irimies, M. and Crainic, L. Behavior of repair/strengthened unreinforced masonry shear walls, in *Proceedings of the Sixth North American Masonry Conference, Drexel University*, 1993, pp. 555–563.

Ismail, F. A., Hakam, A., & Amalia, S. H. (2018). Experimental study on masonry building strengthened with ferrocement layers. *GEOMATE Journal, 14*(45), 84–90.

Jabarov, M., Kozharinov, S., and Lunyov, A. Strengthening of damaged masonry by reinforced mortar layers, *Proceedings of the 7th WCEE, Istanbul, Turkey,* vol. 4, pp. 73–80, 1980.

Jiang, Y. and Yongming, Y. Experimental Study on Masonry Wall Reinforced with Lattice Steel Plates, *Journal of Shenyang Jianzhu University (Natural Science),* vol. 30, no. 1, 2014.

Jiang, H., Liu, X., & Mao, J. (2015). Full-scale experimental study on masonry infilled RC moment-resisting frames under cyclic loads. *Engineering Structures, 91*, 70–84.

Kadam, S. B., Singh, Y., & Li, B. (2014). Strengthening of unreinforced masonry using welded wire mesh and micro-concrete–Behaviour under in-plane action. *Construction and Building Materials, 54*, 247–257.

Kahn, L. Shotcrete retrofit for unreinforced brick masonry, in *8th WCEE*, 1984, vol. 583, p. 590.

Kantharaju, K. V. Kulkarni, S., Chandrashekar, C., Rajappa, G. and Malji, N. Ferrocement components for low cost housing in developing countries, in 26th *Conference on Our World in Concrete Structures*, 2001.

Kumar, G., & Sharma, P. (1976). An Investigation of the ultimate and first crack strength of ferrocement in flexure. *Indian Concrete Journal, 50*(1), 335–344.

Lee, J.-H., Li, C., Oh, S.-H., Yang, W.-J., & Yi, W.-H. (2008). Evaluation of rocking and toe crushing failure of unreinforced masonry walls. *Advances in Structural Engineering, 11*(5), 475–489.

Lizundia, B., Lizundia, B., Longstreth, M., Kren, A. and Abrams, D. P. *Development of procedures to enhance the performance of rehabilitated URM buildings*. US Department of Commerce, National Institute of Standards and Technology, 1997.

Maalej, M., Lin, V., Nguyen, M., & Quek, S. (2010). Engineered cementitious composites for effective strengthening of unreinforced masonry walls. *Engineering Structures, 32*(8), 2432–2439.

Magenes, G., & Calvi, G. M. (1997). In-plane seismic response of brick masonry walls. *Earthquake Engineering & Structural Dynamics, 26*(11), 1091–1112.

Mahmood, H., & Ingham, J. M. (2011). Diagonal compression testing of FRP-retrofitted unreinforced clay brick masonry wallettes. *Journal of Composites for Construction, 15*(5), 810–820.

Mander, J. and Nair, B. "Seismic resistance of brick-infilled steel frames with and without retrofit," *TMS journal,* pp. 24–37, 1994.

Mann, W. Failure of shear-stressed masonry: an enlarged theory, tests and application to shear walls, 1982.

Marzahn, G. The shear strength of dry-stacked masonry walls, *Leipzig Annual Civil Engineering Report (LACER) No,* vol. 3, 1998.

Moghaddam, H. (2004). Lateral load behavior of masonry infilled steel frames with repair and retrofit. *Journal of Structural Engineering, 130*(1), 56–63.

Mustafaraj, E. and Yardım, Y. Usage of ferrocement jacketing for strengthening of damaged unreinforced masonry (URM) walls, 2016.

Naaman, A. E. *Ferrocement and laminated cementitious composites*. Techno press Ann Arbor, 2000.

Nassif, H. H., & Najm, H. (2004). Experimental and analytical investigation of ferrocement–concrete composite beams. *Cement and Concrete Composites, 26*(7), 787–796.

Prawel, S. and Reinhorn, A. "Seismic retrofit of structural masonry using a ferrocement overlay," in *Proceedings of the Third North American Masonry Conference, Arlington, Texas*, 1985, pp. 50–1.

Priestley, M. (1985). Seismic behaviour of unreinforced masonry walls. *Bulletin of the New Zealand Society for Earthquake Engineering, 18*(2), 191–205.

Russell, A., Mahmood, H. and Ingham, J. Pseudo-static in-plane testing of typical New Zealand unreinforced masonry walls, in *Proceedings of the 8th Pacific conference on earthquake engineering, Singapore*, 2007.

Shakib, H., Dardaei, S., Mousavi, M., & Rezaei, M. K. (2016). Experimental and analytical evaluation of confined masonry walls retrofitted with CFRP strips and mesh-reinforced PF shotcrete. *Journal of Performance of Constructed Facilities, 30*(6), 04016039.

Si, Z., Lihua, X., & Dongmin, Y. (2015). Finite element modelling of FRP-reinforced masonry walls under in-plane loadings. *Engineering Mechanics, 32*(12), 233–242.

Taghdi, M., Bruneau, M., & Saatcioglu, M. (2000). Seismic retrofitting of low-rise masonry and concrete walls using steel strips. *Journal of Structural Engineering, 126*(9), 1017–1025.

Tang, C., Luo, R., Cheng, S. and Huang, B. Experimental study of seismic performance of low strength masonry walls reinforced with one-side cement mortar splint, *Journal of Building Structures,* vol. 38, no. 10, 2017.

Thurston, S. and Beattie, G. Seismic performance of New Zealand two storey brick veneer houses, in *Proceedings of the 2009 NZSEE Conference, Christchurch, New Zealand*, 2009.

Trikha, D. Sharma, P. and Johnson, S. Rehabilitation of Corrosion-Damaged Steel Tanks by Ferrocement Treatment at University of Roorkee, in *Proceedings of the 3 rd International Conference on Ferrocement, Roorkee*, 1988, pp. 207–215.

Valvona, F., Toti, J., Gattulli, V., & Potenza, F. (2017). Effective seismic strengthening and monitoring of a masonry vault by using glass fiber reinforced cementitious matrix with embedded fiber bragg grating sensors. *Composites Part b: Engineering, 113*, 355–370.

Yi, T., Moon, F. L., Leon, R. T., & Kahn, L. F. (2006). Lateral load tests on a two-story unreinforced masonry building. *Journal of Structural Engineering, 132*(5), 643–652.